



# Arbor-shrub mixed vegetation restoration strategies cause greater increases in plant-derived carbon than microbial-derived carbon in limestone hills

Longyan Shi <sup>a,b</sup>, Tiandong Xu <sup>a,b</sup>, Yutian Zhang <sup>a,b</sup>, Linjing Zhang <sup>a,b</sup>, Hongbo Tao <sup>c</sup>, Jiahao Zhao <sup>d</sup>, Junjie Li <sup>a,b</sup>, Chenyi Yu <sup>a,b</sup>, Xinli Chen <sup>e</sup>, Qingwei Guan <sup>a,b,\*</sup>

<sup>a</sup> Collaborative Innovation Center of Sustainable Forestry in Southern China, Nanjing 210037, China

<sup>b</sup> College of Ecology and the Environment, Nanjing Forestry University, Nanjing 210037, China

<sup>c</sup> Xuzhou Tongshan District Forestry Technical Guidance Station, Xuzhou 221100, China

<sup>d</sup> College of Horticulture, Nanjing Agricultural University, Nanjing 210095, China

<sup>e</sup> State Key Laboratory of Subtropical Silviculture, Zhejiang A&F University, Hangzhou 311300, China



## ARTICLE INFO

### Keywords:

Vegetation restoration strategies  
Mixed forest  
Monoculture forest  
Plant-derived carbon  
Microbial-derived carbon  
Limestone hills

## ABSTRACT

Both mixed and monoculture strategies significantly influence the sequestration of soil organic carbon (SOC) in limestone hills and are crucial for mitigating climate warming. However, the mechanisms underlying the differential responses of plant- and microbial-derived SOC in these forests remain poorly understood. In this study, lignin phenols and amino sugars were measured to explore the differences in plant- and microbial-derived carbon between arbor-shrub mixed forests and monoculture forests established on a limestone hill in 2012. The results indicated that mixed forests of *Acer pictum* × *Ligustrum quihoui* and *Pistacia chinensis* × *Pyracantha fortuneana* increases plant-derived carbon contents by 73.46 % and 40.41 %, respectively, with corresponding contributions to SOC rising by 10.18 % and 4.98 %, compared to their respective monoculture forests (*Acer pictum* and *Pistacia chinensis*). In contrast, microbial-derived carbon increased by 7.65 % and 22.22 %, while their contributions to SOC decreased by 9.39 % and 1.05 %, respectively. Notably, plant-derived carbon exhibited higher increases than microbial-derived carbon, underscoring its more prominent influence on soil carbon sequestration. Arbor-shrub mixed strategies enhanced both plant- and microbial-derived carbon content by affecting the soil bulk density, total nitrogen and phosphorus content, fine root biomass, fungal diversity, and β-glucosidase and sucrase enzyme activities, thereby contributing to an increase in SOC levels. Given the profound influence of plant- and microbial-derived carbon on carbon sequestration, these findings underscore the critical importance of prioritizing arbor-shrub mixed vegetation afforestation strategies for limestone hills.

## 1. Introduction

Soil is the largest active carbon (C) pool in terrestrial ecosystems and stores approximately four times more C than vegetation and three times more C than the atmosphere (Lal et al., 2021; Feng et al., 2024). Consequently, the scale and stability of forest soil C play a critical role in mitigating global climate change. Plant-derived C primarily consists of residues such as lipids, cutin, and lignin generated during the decomposition of plant litter (Otto et al., 2005; Otto et al., 2006; Zhou et al., 2022). In contrast, microbial-derived C primarily consists of microbial lipid compounds and microbial remnants (Feng et al., 2007; Yang et al.,

2024). Both plant- and microbial-derived C exhibit biochemical recalcitrance, which prevents them being decomposed by microorganisms, thereby enhancing the storage and stability of soil organic carbon (SOC) (Gunina et al., 2022). Given that plant- and microbial-derived C present varying levels of efficiency and durability in generating stable SOC (Whalen et al., 2022), the dynamic variations and driving factors underlying plant-derived and microbial-derived C must be better understood to elucidate the sequestration mechanisms of SOC (Chen et al., 2021; Liang, 2020; Liang and Zhu, 2021; Whalen et al., 2022; Yang et al., 2024; Zhang et al., 2023).

Mixed and monoculture forests are commonly used for vegetation

\* Correspondence to: No. 159 Longpan Road, Nanjing, Jiangsu 210037, China.

E-mail addresses: [Sly9990329@163.com](mailto:Sly9990329@163.com) (L. Shi), [xutiandong200101@163.com](mailto:xutiandong200101@163.com) (T. Xu), [zhangyutian0411@163.com](mailto:zhangyutian0411@163.com) (Y. Zhang), [1501612003@qq.com](mailto:1501612003@qq.com) (L. Zhang), [thongbo2006@163.com](mailto:thongbo2006@163.com) (H. Tao), [jhzhaoy@njau.edu.cn](mailto:jhzhaoy@njau.edu.cn) (J. Zhao), [junjie@njfu.edu.cn](mailto:junjie@njfu.edu.cn) (J. Li), [yuchenyi0914@163.com](mailto:yuchenyi0914@163.com) (C. Yu), [xinlichen@zafu.edu.cn](mailto:xinlichen@zafu.edu.cn) (X. Chen), [guanjanpan999@163.com](mailto:guanjanpan999@163.com) (Q. Guan).

restoration (Li et al., 2022; Pretzsch and Schutze, 2016; Richards et al., 2010). Several studies have demonstrated that both mixed and monoculture forests can significantly influence soil plant-derived and microbial-derived C, thereby regulating the SOC pool (Angst et al., 2021; Jia et al., 2021; Jing et al., 2024; Qin et al., 2024a). In the subtropical region, *Phyllostachys edulis* and evergreen broadleaf mixed forests showed significantly increased microbial-derived C accumulation compared to *Phyllostachys edulis* monoculture forests (Shao et al., 2024). Similarly, *Alniphyllum fortunei* and *Larix gmelinii* mixed forests promoted amino sugar and microbial necromass C accumulation and subsequently enhanced the stability of SOC compared to *Alniphyllum fortunei* forests (Jing et al., 2024). Jia et al. (2021) suggested that mixed forests with higher biodiversity can enhance the contributions of both plant-derived and microbial-derived C, whereas Qin et al. (2024b) found that mixed forests did not significantly alter the content of microbial-derived C or its contribution to the SOC pool. However, evidence on the impact of mixed and monoculture forests on soil plant-derived and microbial-derived carbon remains insufficient.

The prevailing view indicated that plant-derived C components (such as lignin) serve as primary contributors to stabilized SOC (Cotrufo et al., 2019; Lavallee et al., 2020; Ma et al., 2018). However, despite its recalcitrance, lignin may still undergo gradual decomposition by soil microbes over time (Cotrufo et al., 2013). In contrast, soil microorganisms can convert both plant C and their own biomass into microbial necromass while decomposing plant compounds (Liang, 2020; Liang and Zhu, 2021), and this necromass then accumulates on soil mineral surfaces or binds with minerals, thus forming more stable SOC (Castellano et al., 2015; Cotrufo et al., 2013; Kallenbach et al., 2016; Liang et al., 2019; Ma et al., 2018; Shao et al., 2019). From this perspective, microbial-derived C may play a more significant role than plant-derived C in the long-term stability of SOC (Cotrufo et al., 2013; Castellano et al., 2015; Miltner et al., 2012; Liang et al., 2017). Nevertheless, plant-derived C serves as the primary energy source for soil microorganisms (Fu et al., 2022); however, because of its irreversible sorption onto minerals, its role in the stabilization of SOC may be underestimated (Angst et al., 2021; Wang et al., 2021; Whalen et al., 2022). Consequently, determining the respective contributions of plant-derived and microbial-derived C to SOC is essential for understanding how mixed and monoculture forests affect SOC sequestration.

The formation of plant-derived and microbial-derived C is influenced by a multitude of factors, including plant substrates, soil organic matter, environmental conditions, and microbial community structure (Angst et al., 2021; Hao et al., 2025; Huang et al., 2023). Different vegetation restoration strategies can alter plant C inputs and the physical, chemical, and biological properties of soils, thereby influencing the contributions of plant- and microbial-derived C to SOC and the mechanisms underlying these processes. Zhang et al. (2022) demonstrated that afforestation strategies on the Loess Plateau increase microbial-derived C rather than plant-derived C through enhancing both the quantity and quality of litter inputs, which promote the allocation of SOC to stable aggregates and ultimately enhance storage and stability of SOC. In contrast, Zhao et al. (2024) revealed that soil pH, SOC content, exchangeable calcium, gram-negative bacterial biomass, and C-to-nitrogen (C/N) ratios affect the SOC pool by modulating plant-derived C. These findings reveal that the key factors influencing plant- and microbial-derived C must be identified to gain a more comprehensive understanding of SOC sequestration across different vegetation restoration strategies. Nevertheless, few studies have explored the key factors affecting plant- and microbial-derived C under mixed versus monoculture vegetation restoration strategies in limestone hills.

Limestone hills are globally distributed and represent critical ecosystems characterized by inherently low soil fertility, a limited water-holding capacity, and fragmented vegetation cover (Liu et al., 2020; Zhang et al., 2024). Previous research has confirmed that arbor-shrub mixed forests significantly enhance SOC storage and stability in limestone hills relative to monoculture forests (Shi et al., 2025).

Nevertheless, the specific mechanisms by which these vegetation restoration strategies impact the dynamics of plant-derived and microbial-derived C and subsequently influence SOC sequestration remain poorly understood. This significant knowledge gap impedes a more comprehensive understanding of how mixed and monoculture vegetation restoration strategies regulate the potential for SOC sequestration in limestone hills.

To address these knowledge shortfalls, this study used lignin phenols and amino sugars as biomarkers to quantify the soil plant- and microbial-derived C, respectively; compared the contributions of these components to SOC; and identified the associated influencing factors. The objectives of this research were to (i) quantify the contents and contributions of plant- and microbial-derived components (bacterial or fungal) to SOC under different vegetation restoration strategies; and (ii) identify the key factors and underlying mechanisms that influence plant- and microbial-derived C. The findings underscore the pronounced advantages of arbor-shrub mixed forests compared to monoculture forests on plant- and microbial-derived C sequestration in limestone hills and offer guidance for implementing afforestation and ecological restoration practices in limestone hills.

## 2. Materials and methods

### 2.1. Site description

A field investigation was carried out at Zhaotuan Forest Farm (geographical coordinates: 34°10'–34°12'N, 117°27'–117°29'E; altitude: 184 m), located on the outskirts of Xuzhou City, Jiangsu Province, China (as illustrated in Fig. 1). This area is characterized by a warm-temperate semi-humid monsoon climate. The mean annual temperature in this region is 13.9 °C, and the annual precipitation fluctuates between 800 and 900 mm. The soil in this area is categorized as a Mollisol according to the USDA soil taxonomy and developed via limestone leaching processes. Thus, substantial limestone content is observed within the soil profile up to a depth of approximately 20–25 cm. However, the nutrient levels in the soil are relatively low, and the region frequently experiences drought events and water scarcity.

Since 2012, a vegetation restoration initiative has been implemented in this area employing a block-mixed planting strategy. Tree species, including *Acer pictum* subsp. *mono* (Maxim.) H. Ohashi and *Pistacia chinensis* Bunge, as well as shrub species, including *Ligustrum quihoui* Carr. and *Pyracantha fortuneana* (Maxim.) H. L. Li, have been cultivated either in monoculture stands or in mixed plantations. Identical vegetation restoration approaches have been adopted in non-contiguous plots within the region. Location and basic information of the study area are shown in Fig. 1.

For this study, three randomized blocks of *Acer pictum* monoculture forests (Ap), *Pistacia chinensis* monoculture forests (Pc), *Acer pictum* × *Ligustrum quihoui* mixed forests (ApLq), and *Pistacia chinensis* × *Pyracantha fortuneana* mixed forests (PcPf) were established in April 2023 based on similarities in the slope, growth, and density characteristics. A 25 m × 25 m fixed plot was established for each of the four forest types in each randomized block, resulting in a total of 12 plots. To mitigate spatial variability, a minimum boundary distance of over 30 m was maintained between adjacent plots. Basic information on the sample plots is presented in Table 1.

### 2.2. Soil and plant sampling and processing

In each plot, seven soil samples were collected in an "S"-shaped pattern at each depth using a 5-cm inner-diameter metallic auger. Samples from the same soil layer were combined into a composite sample for lab analysis. Each composite sample was sieved through a 2-mm mesh to exclude visible extraneous matter. The sieved samples were split into two portions, with one stored at -70 °C for soil microbial

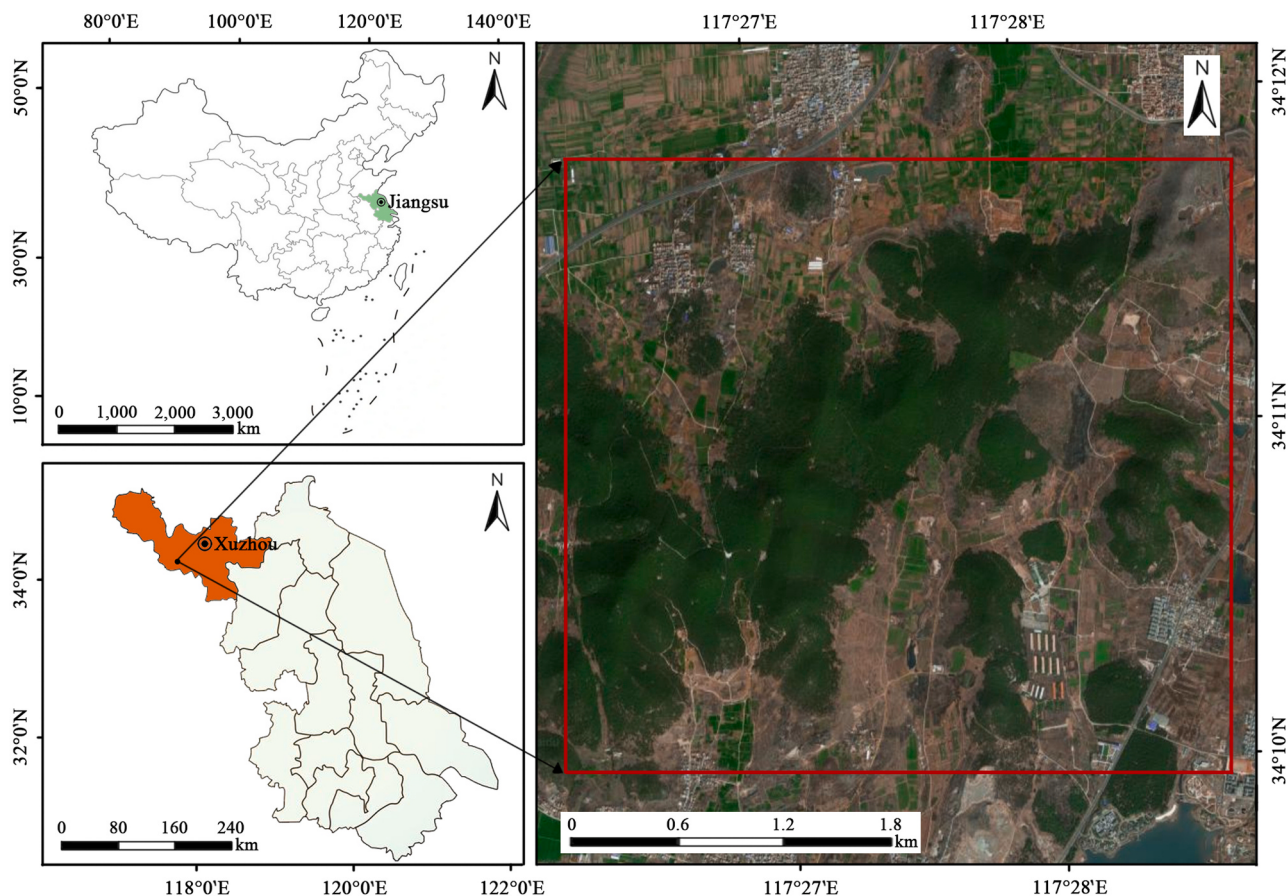


**Fig. 1.** Location and basic information of the study area.

**Table 1**  
Basic information of sample plots.

Restoration strategies	Longitude/Latitude	Altitude (m)	Slope (°)	Tree species composition	Stand age (years)	Stand density (stem ha <sup>-1</sup> )		Mean DBH (cm)	Mean height (m)
						Individual population of tree	Individual population of shrub		
Ap	117°28'42.2"E 34°11'25.2"N	136	18	<i>Acer pictum</i>	13	1100	0	6.56 ± 0.26	4.58 ± 0.47
ApLq	117°27'46.3"E 34°10'24.6"N	130	15	<i>Acer pictum</i> × <i>Ligustrum quihoui</i>	13	1075	4300	9.91 ± 0.65	5.91 ± 0.43
Pc	117°28'39.8"E 34°11'26.8"N	122	15	<i>Pistacia chinensis</i>	13	1100	0	7.93 ± 1.36	5.14 ± 0.18
PcPf	117°28'39.6"E 34°10'26.2"N	121	16	<i>Pistacia chinensis</i> × <i>Pyracantha fortuneana</i>	13	1050	4200	9.32 ± 0.34	6.3 ± 0.44

community analysis and the other air-dried at room temperature for SOC fraction and physicochemical property analysis.

For each 25 m × 25 m experimental plot, a five-point sampling layout was implemented to delineate five 1 m × 1 m subplots. Within each subplot, a 20 cm × 20 cm frame was positioned to define the boundaries for litterfall collection. The dead branches and leaves at the periphery of the frame were pruned, and the litterfall within the frame was collected transported to the laboratory. Moreover, in each 25 m × 25 m plot, three typical standard trees were chosen according to the mean values of diameter at breast height and tree height. Uniformly spaced sampling points were established 30 cm away from the base of each tree trunk. Following the removal of the surface litter layer, a root-sampling auger was employed to obtain three undisturbed soil cores from both the 0–10 cm and 10–20 cm soil strata. All fine roots (defined as those with a diameter ≤ 2 cm) present within the soil cores were transported to the laboratory.

### 2.3. Soil and plant characteristics analysis

Soil bulk density (BD) was determined using the cutting ring method (5.0 cm diameter × 5.0 cm height). Soil pH was measured using the potentiometric method as described by Haghverdi and Kooch (2019). Total C (TC) and total N (TN) contents were quantified using an elemental analyzer (Elementar Vario EL, Germany), while total phosphorus (TP) content was measured using the molybdenum-antimony colorimetric method (Sheng et al., 2018). Litterfall biomass (LB) and fine root biomass (FRB) were determined using the drying and weighing method. The lignin composition of aboveground litterfall and fine roots was analyzed using the alkaline CuO oxidation method (Duboc et al., 2014). Soil enzymatic activities, including β-glucosidase (BG) and sucrase (SC), were measured using a microplate fluorescence assay with a multifunctional enzyme reader (Tecan Infinite 200 PRO, Switzerland).

Since the soil pH was greater than 7, the SOC content was determined

using the sulfuric acid-potassium dichromate heating method (Bao, 2000). Microbial biomass C (MBC) content was determined using the chloroform fumigation-K<sub>2</sub>SO<sub>4</sub> extraction method (Jenkinson, 1988) and calculated using the formula:

$$\text{MBC (mg kg}^{-1}\text{)} = (\text{C extracted from fumigated soil} - \text{C extracted from non-fumigated soil}) \times 0.45^{-1} \quad (1)$$

Dissolved organic carbon (DOC) content was determined by a TOC analyzer (TOC-VCPN, Shimadzu, Japan) after extraction using a K<sub>2</sub>SO<sub>4</sub> solution (0.5 mol L<sup>-1</sup>) (Dong et al., 2009).

Microbial DNA was extracted using an OMEGA Soil DNA Kit (D5635-02, Omega Bio-tek, Norcross, GA, USA) according to the manufacturer's instructions. The bacterial 16S rRNA gene's hypervariable V3–V4 region was amplified with primers 338 F and 806 R (Klindworth et al., 2013), and the fungal internal transcribed spacer (ITS) region was amplified with primers ITS1 and ITS4 (Edgar, 2013). Subsequently, the polymerase chain reaction (PCR) amplification process was carried out. PCR amplicons were purified using Vazyme VAHTSTM DNA Clean Beads (Vazyme, Nanjing, China) and quantified with the Quant-iT PicoGreen dsDNA Assay Kit (Invitrogen, Carlsbad, CA, USA). The purified PCR products were pooled equimolarly and sequenced on the Illumina NovaSeq platform using a NovaSeq 6000 SP Reagent Kit (500 cycles) at Shanghai Personal Biotechnology Co., Ltd. (Shanghai, China).

#### 2.4. Determination of lignin phenols and plant-derived C

The estimation of plant-derived C primarily relies on the quantification of lignin phenols. The measurement of lignin phenol content was conducted following the method described by Hedges and Ertel (1982), which involves CuO oxidation and solid-phase extraction to determine the concentrations of cinnamyl-type (C), syringyl-type (S), and vanillyl-type (V) monomers in the soil. Briefly, approximately 0.5 g of soil was weighed and placed into a polytetrafluoroethylene (PTFE) reaction vessel, followed by the sequential addition of 1 g of CuO, 0.1 g of Fe(NH<sub>4</sub>)<sub>2</sub>(SO<sub>4</sub>)<sub>2</sub>·6H<sub>2</sub>O, and 15 mL of 2 mol/L NaOH solution. The air inside the reaction vessel was purged with N gas for 15 min to ensure an inert atmosphere before the vessel was sealed. The sealed vessel was then heated in an oven at 170 °C for 2.5 h to facilitate hydrolysis. The hydrolyzed soil samples were treated with N, O-bis-(trimethylsilyl) trifluoroacetamide (BSTFA) and pyridine at 60 °C for 3 h to produce derivatives of trimethylsilyl (TMS) (Ma et al., 2018). Gas chromatography (GC, Agilent Technologies, USA) was used to quantify the derivatives (Xia et al., 2021). The content of lignin phenol was defined as the sum of the C-, S-, and V-type phenol contents. Because approximately 33.33 % of the V-type phenols, 90 % of the S-type phenols and 100 % of the C-type phenols were hydrolyzed by CuO, the content of plant-derived C was estimated using the following equation (Chen et al., 2021; Chen et al., 2024b):

$$\text{Plant-derived C} = (V \times 3 + S/0.9 + C)/0.08 \quad (2)$$

where C, S, and V denote the C contents related to C-, S-, and V-type phenols (g kg<sup>-1</sup>), respectively; and 0.08 denotes the minimal lignin content of the plant residues. The contribution of plant-derived C to SOC = plant-derived C / SOC.

#### 2.5. Determination of amino sugars and microbial-derived C

Microbial-derived C is primarily estimated through the quantification of amino sugars. The amino sugar content was determined following the method described by Joergensen (2018). Briefly, approximately 0.5 g of air-dried soil sample was weighed and subjected to hydrolysis by adding 10 mL of 6 mol L<sup>-1</sup> HCl solution, followed by incubation at 105 °C for 8 h in an oven. After hydrolysis, HCl was removed using an evaporator, as outlined by Qin et al. (2024a). Subsequently, GC (Agilent Technologies, USA) was performed to quantify

the amino sugar extract contents according to the different peak times of the different amino sugar components in the standard sample (Liang et al., 2019). The total amino sugar content is expressed as the sum of glucosamine (GlcN), mannosamine (ManN), galactosamine (GalN), and muramic acid (MurA). The formulae in Hu et al. (2024) were used to calculate fungal necromass C (FNC), bacterial necromass C (BNC), and microbial-derived C.

$$\text{FNC} = (\text{GlcN} - 1.16 \times \text{MurA}) \times 10.8 \quad (3)$$

$$\text{BNC} = \text{MurA} \times 31.3 \quad (4)$$

$$\text{Microbial-derived C} = \text{FNC} + \text{BNC} \quad (5)$$

where GlcN and MurA denote the content of glucosamine and muramic acid (g kg<sup>-1</sup>), respectively. The contribution of microbial-derived C to SOC = microbial-derived C / SOC (Liang et al., 2019).

#### 2.6. Statistical analyses

SPSS 22 software (IBM SPSS Statistics, USA) was employed for initial data analysis. The Shapiro-Wilk test and Levene's test were employed to assess the normality of residues and homogeneity of variance for various soil properties, litterfall and fine root characteristics, and lignin phenol, plant-derived C, amino sugars, fungal necromass C, bacterial necromass C, and microbial-derived C contents, as well as (Ad/AI) V and (Ad/AI) S. Subsequently, independent-samples t-tests, one-way analysis of variance (ANOVA), and least significance difference (LSD) multiple-comparison post-hoc tests were conducted to analyze the significant differences among the data of the two soil layers or four vegetation restoration strategies. Statistical significance was set at  $p < 0.05$ . To mitigate multicollinearity among the explanatory variables, collinearity diagnostics was performed to exclude strongly correlated variables ( $|r| > 0.8$ ) (Delgado-Baquerizo et al., 2017; Zhao et al., 2024).

The remaining data were then transferred to R 4.4.1 software for further analysis and graphical visualization. The Mantel test and Pearson's correlation analysis were implemented using the R package "vegan" to investigate the associations between soil properties, litterfall and fine root characteristics, and lignin phenol and amino sugar content and determine their impacts on plant-derived C and microbial-derived C. Based on the Mantel test results, we developed a structural equation model (SEM) to examine the direct and indirect drivers of soil properties and litterfall and fine root characteristics on plant-derived C, microbial-derived C, and SOC. SEM was implemented using the R package "lavaan." Chi-square tests (Chi-sq), P-values, comparative fit index (CFI), goodness-of-fit index (GFI), and standardized root mean square residual (SRMR) were used to evaluate the final model. Statistical significance was set at  $p < 0.05$ .

### 3. Results

#### 3.1. Differences in amino sugars, FNC, BNC, and microbial-derived C

The results of the total amino sugar, FNC, BNC, and microbial-derived C content analyses are presented in Fig. 2. In the 0–10 cm soil layer, the amino sugar, FNC, BNC, and microbial-derived C contents in the ApLq forest were 14.60 %, 3.48 %, 12.70 %, and 16.64 % higher than those of the Ap forest, respectively ( $p < 0.05$ ). Similarly, compared to the Pc forest, the above metrics showed increases of 37.97 %, 54.11 %, 40.74 %, and 37.08 % in the PcPf forest, respectively ( $p < 0.05$ ). In the 10–20 cm soil layer, the BNC content in the ApLq and PcPf forests was 45.73 % and 12.90 % higher than that in the Ap and Pc forests, respectively ( $p < 0.05$ ) (Fig. 2c). However, significant differences were not observed between the two groups of forests in terms of amino sugar content, FNC content, and microbial-derived C content in the 10–20 cm soil layer. Overall, the average amino sugar, FNC, BNC, and microbial-derived C contents were significantly higher in the mixed

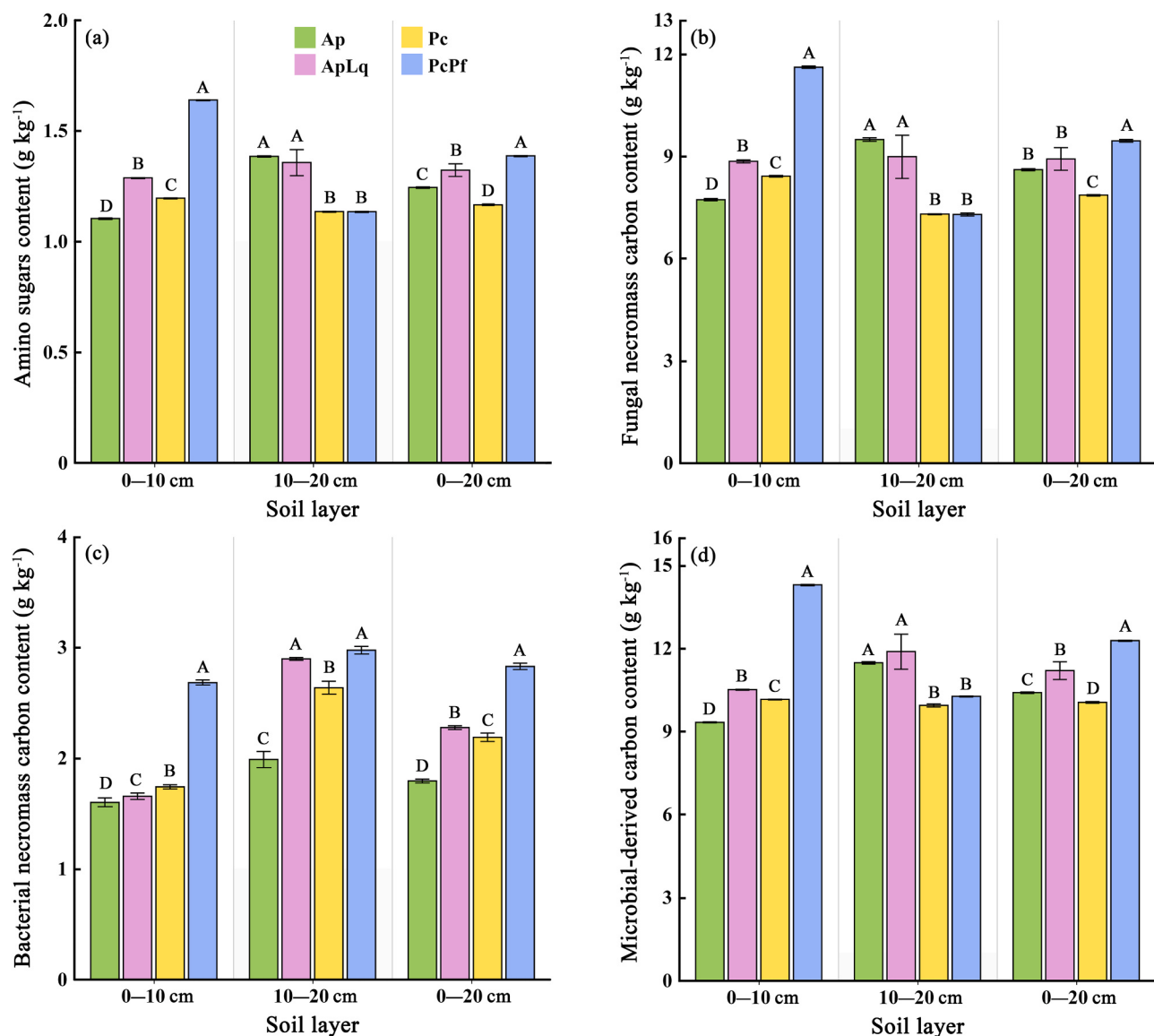


**Fig. 2.** Changes in amino sugar (a), fungal necromass carbon (b), bacterial necromass carbon (c), and microbial-derived carbon (d) contents in the four vegetation restoration strategies. Ap, *Acer pictum* monoculture forest; ApLq, *Acer pictum* × *Ligustrum quihoui* mixed forest; Pc, *Pistacia chinensis* monoculture forest; Pcpf, *Pistacia chinensis* × *Pyracantha fortuneana* mixed forest. Different uppercase letters indicate significant differences between different vegetation types in the same soil layer ( $p < 0.05$ ).

forests than the pure forests.

### 3.2. Differences in lignin phenol and plant-derived C

Compared to the Ap forest, the ApLq forest showed an average increase of 71.95 % and 73.47 % in lignin phenol and plant-derived C contents, respectively ( $p < 0.05$ ) (Figs. 3a, 3b). Specifically, in the 0–10 cm soil layer, these values increased by 59.85 % and 65.56 %, while in the 10–20 cm soil layer, they increased by 92.93 % and 87.32 % ( $p < 0.05$ ). Similarly, compared to the Pc forest, the Pcpf forest exhibited an average increase of 35.32 % and 40.41 % in lignin phenol and plant-derived C contents, respectively ( $p < 0.05$ ). In the 0–10 cm soil layer, these values increased by 25.85 % and 30.14 %, whereas in the 10–20 cm soil layer, they increased by 50.68 % and 57.02 % ( $p < 0.05$ ). The lignin phenol and plant-derived C contents demonstrated a clear decreasing trend with increasing soil depth.

The (Ad/Al) V value was significantly higher across all soil layers in the ApLq forest compared to the Ap forest ( $p < 0.05$ ), while the (Ad/Al) S value exhibited a significant decrease in the 10–20 cm soil layer

( $p < 0.05$ ) but showed no significant difference in the 0–10 cm soil layer ( $p > 0.05$ ) (Figs. 3c, 3d). Conversely, the (Ad/Al) V value in the Pcpf forest was significantly lower than that in the Pc forest across all soil layers ( $p < 0.05$ ), while the (Ad/Al) S value showed inconsistent variations across the soil layers ( $p > 0.05$ ).

### 3.3. Differences in the relative contribution of plant- and microbial-derived C to SOC

Compared with the Ap forest, the ApLq forest demonstrated an increase in the contribution of plant-derived C to SOC from 39.65 % to 49.83 % and a decrease in the contribution of microbial-derived C from 42.65 % to 33.26 % (Figs. 4a, 4b). Additionally, the contribution of FNC to SOC declined from 82.76 % to 79.68 %, whereas the contribution of BNC increased from 17.24 % to 20.32 %. Similarly, relative to the Pc forest, the Pcpf forest showed an increase in the contribution of plant-derived C to SOC from 39.5 % to 44.48 % but a slight decline in the contribution of microbial-derived C from 52.25 % to 51.2 % (Figs. 4c, 4d). The contribution of FNC to SOC decreased from 78.24 % to

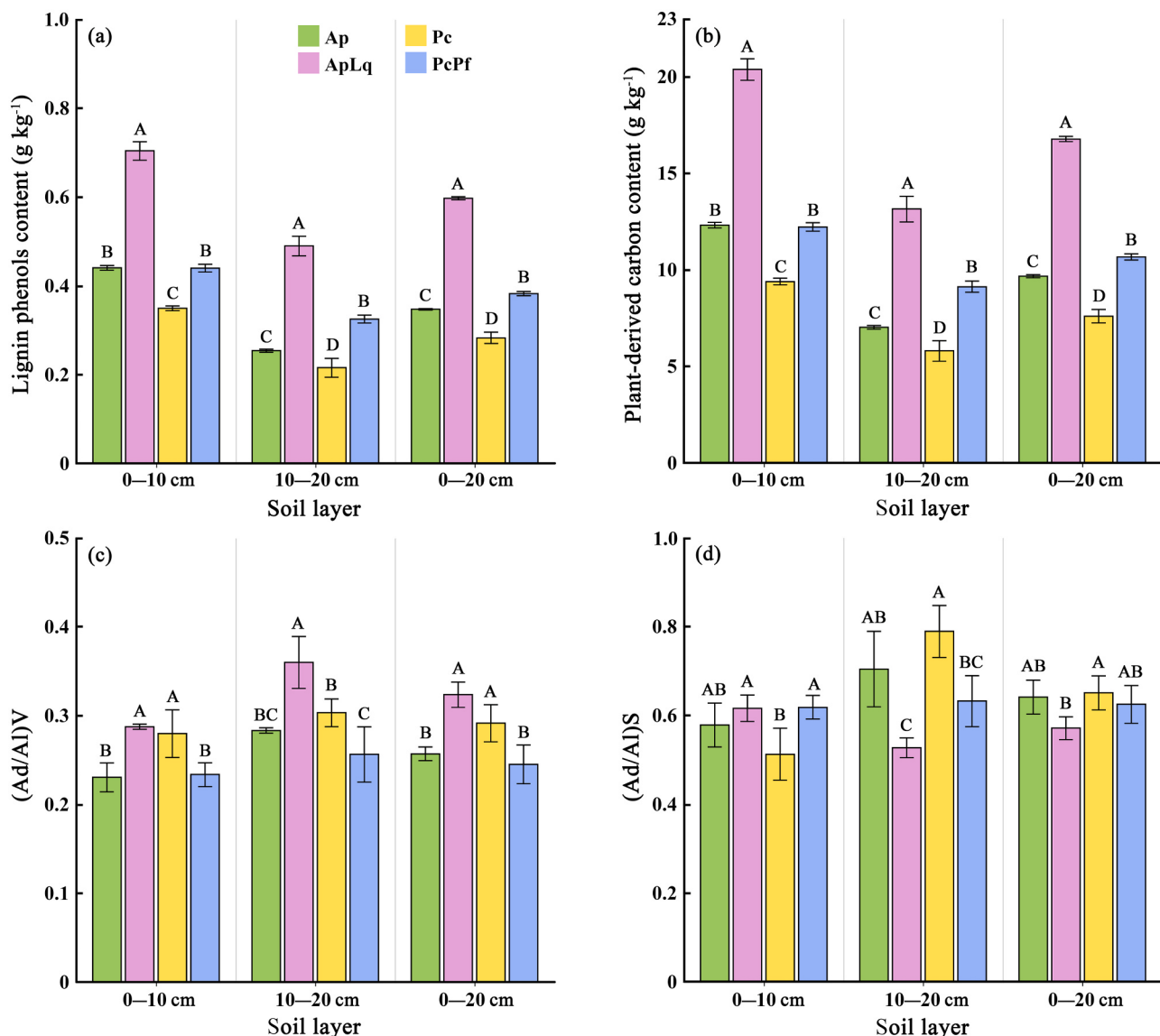


**Fig. 3.** Changes in lignin phenol contents (a), plant-derived carbon contents (b), acid to aldehyde (Ad/AI) ratios of V-type phenols (c), and acid to aldehyde (Ad/AI) ratios of S-type phenols (d) in the four vegetation restoration strategies. Ap, *Acer pictum* monoculture forest; ApLq, *Acer pictum* × *Ligustrum quihoui* mixed forest; Pc, *Pistacia chinensis* monoculture forest; Pcpf, *Pistacia chinensis* × *Pyracantha fortuneana* mixed forest. Different uppercase letters indicate significant differences between different vegetation types in the same soil layer ( $p < 0.05$ ).

76.98 %, while the contribution of BNC increased from 21.76 % to 23.02 %. Overall, arbor-shrub mixed forests significantly enhanced the contributions of plant-derived C and BNC to SOC compared with monoculture forests.

#### 3.4. Ability of soil and plant properties to regulate plant- and microbial-derived C and their contributions to SOC

The Mantel test was used to investigate the effects of soil physico-chemical properties, C fractions, enzyme activities, microbial diversity, plant characteristics, lignin phenols, and amino sugars on plant-derived C and microbial-derived C accumulation (Fig. 5). The accumulation of plant-derived C was strongly regulated ( $p < 0.01$ ) by TN, FFRB, BG, SC, SOC, MBC, (Ad/AI) V, and lignin phenols, whereas it was significantly influenced ( $p < 0.05$ ) by BD, DOC, (Ad/AI) S, amino sugars and FNC. Similarly, microbial-derived C accumulation was strongly regulated ( $p < 0.01$ ) by FR-L/N, F-Chao1, MBC, DOC, amino sugars, FNC, and BNC.

Based on these key regulatory factors, SEM (Fig. 6) explained 97 % of

the total variation in SOC accumulation driven by different vegetation restoration strategies. Arbor-shrub mixed vegetation restoration forests and monoculture plantations influenced SOC accumulation primarily by directly altering the soil BD, TN and TP contents, and their stoichiometric ratios. These changes impacted fine root biomass, thereby modulating lignin phenol levels and plant-derived C accumulation, which emerged as the dominant pathways regulating the changes in SOC content. Another critical pathway involved the direct or indirect influence of vegetation restoration strategies on fungal diversity and the activity of extracellular enzymes such as BG and SC, which regulated the production of microbial-derived C and the changes of SOC content. Furthermore, SEM and standardized total effects from SEM also demonstrated that the contribution of plant-derived C to SOC content was greater than that of microbial-derived C.

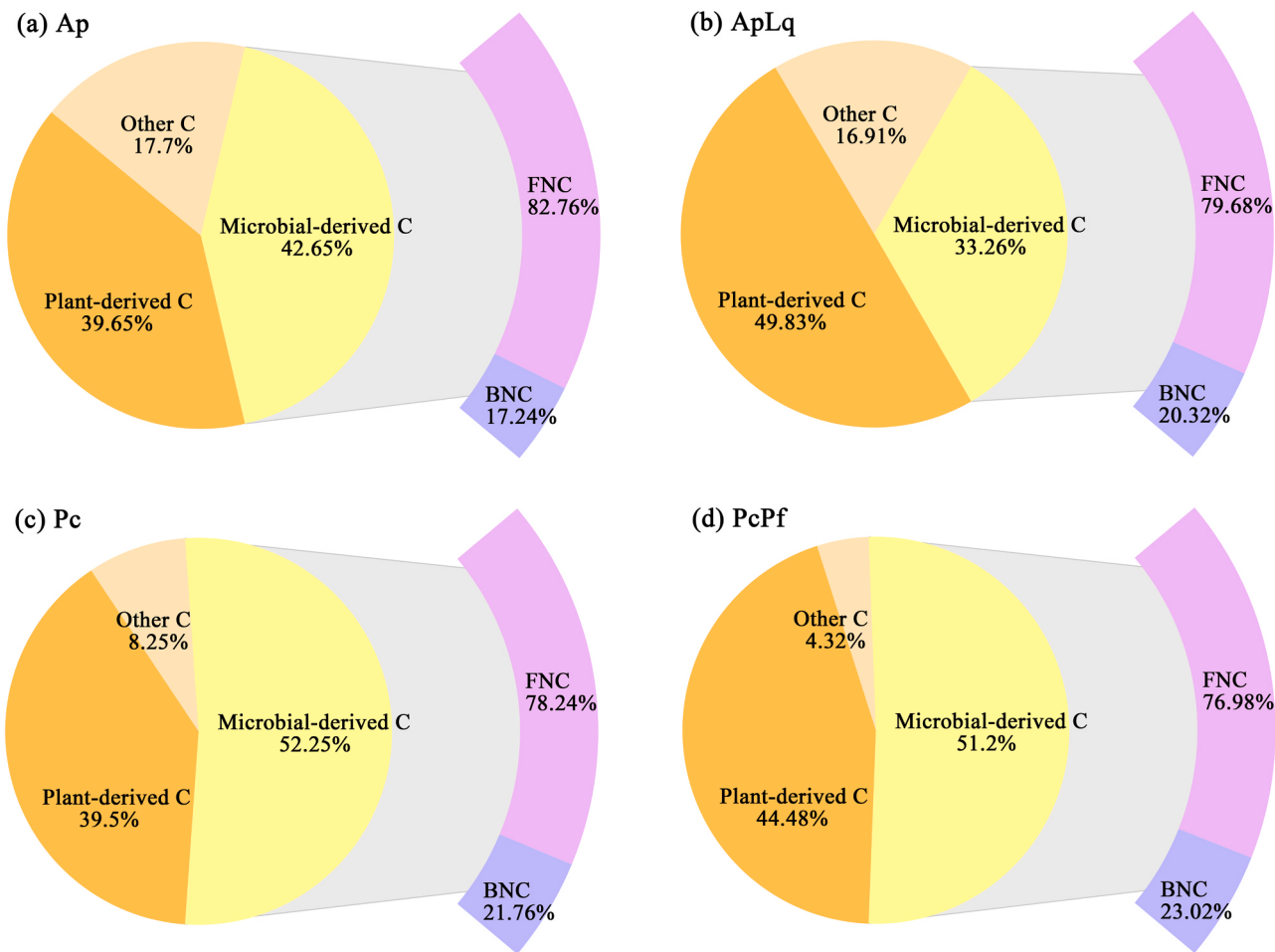


**Fig. 4.** Pie chart of the contributions of microbial, plant, fungal, and bacterial necromass carbon to soil organic carbon in the four vegetation restoration strategies. Ap, *Acer pictum* monoculture forest; ApLq, *Acer pictum* × *Ligustrum quihoui* mixed forest; Pc, *Pistacia chinensis* monoculture forest; Pcpf, *Pistacia chinensis* × *Pyracantha fortuneana* mixed forest.

#### 4. Discussion

##### 4.1. Arbor-shrub mixed and monoculture forests influence amino sugars and microbial-derived C

Our results revealed that the contents of total amino sugars, FNC and microbial-derived C in the two arbor-shrub mixed stands (ApLq and Pcpf) were significantly higher than those in the monoculture stands (Ap and Pc) (Fig. 2). The accumulation of these components was influenced by factors such as FR-L/N, F-Chao1, B-Chao1, MBC, and DOC (Fig. 5). Amino sugars originate from the hydrolysis of microbial cell wall components, such as fungal chitin, bacterial peptidoglycan, and glycoproteins (Hu et al., 2020). Theoretically, forests that provide a more abundant C source to microorganisms and stimulate greater microbial C use efficiency (CUE) are expected to incorporate more metabolic byproducts into microbial residues (Bradford et al., 2013; Sokol et al., 2019). Consequently, such stands are more likely to accumulate higher amounts of amino sugars and microbial-derived C. The ApLq and Pcpf stands effectively enhanced forest growth, as evidenced by increases in mean height and mean diameter at breast height (Table 1). These improvements facilitated higher photosynthetic efficiency and fine root turnover (Lange et al., 2015), thereby increasing the biomass of litter and fine roots, which provided more labile substrates in the form of DOC (Table 2; Jia et al., 2021). DOC has been shown to enhance microbial CUE and stimulate microbial residue accumulation in mineral soils (Cotrufo et al., 2013).

Previous models and laboratory incubation studies have

demonstrated that high-quality substrates, characterized by low C/N ratios and low lignin-to-N (L/N) ratios, promote the accumulation of more microbial-derived SOM compared to low-quality substrates (Castellano et al., 2015; Córdova et al., 2018). This provides a further explanation for the observed increase in amino sugars and microbial-derived C in the arbor-shrub mixed forests. MBC exhibited a significant positive correlation with the contents of amino sugar and microbial-derived C (Ding et al., 2020) because higher-quality plant substrates (with lower L/N ratios) enhanced fungal and bacterial diversity and activity, thereby stimulating microbial growth. Elevated MBC is particularly conducive to the formation of microbial residues through the continuous microbial turnover and burial effect (Han et al., 2024; Wu et al., 2024). These findings underscore the importance of arbor-shrub mixed forests in improving SOC stabilization through microbial pathways.

Consistent with the findings of most previous studies (He et al., 2022; Zhao et al., 2024), our results showed that the FNC content exceeded the BNC content across the four vegetation restoration forests. This can be attributed to several factors. First, fungal biomass generally surpasses bacterial biomass in most ecosystems (He et al., 2022; Wang et al., 2021), and fungi possess a superior capacity to decompose plant residues through the secretion of extracellular enzymes such as β-glucosidase (BG) and sucrase (SC) (Deng et al., 2021; Luo et al., 2023; Xia et al., 2020). Second, organic matter is more readily transformed into fungal biomass through intracellular turnover pathways compared to bacterial biomass (Liang et al., 2017), thereby facilitating the formation of fungal residues. Moreover, fungi exhibit a higher CUE than bacteria

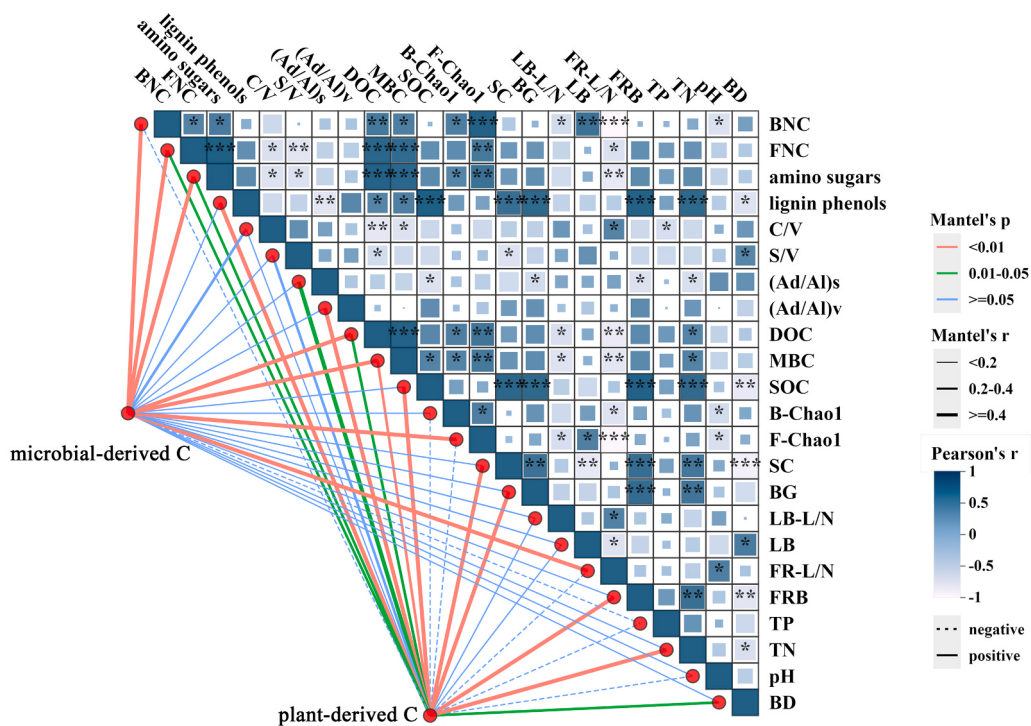


**Fig. 5.** Correlations between soil physicochemical properties, carbon fractions, enzyme activities, microbial diversity, and plant-derived carbon and microbial-derived carbon. Note: Edge width corresponds to the Mantel's  $r$  statistics for the corresponding distance correlations, and edge color denotes the significance. The positive and negative relationships between two variables are represented by dark blue and light blue, respectively. The deeper the color, the stronger the relationship. ns indicates no significant difference; \*  $p < 0.05$ ; \*\*  $p < 0.01$ ; \*\*\*  $p < 0.001$ . BD, soil bulk density; pH, soil pH; TN, soil total nitrogen content; TP, total phosphorus content; SOC, soil organic carbon content; MBC, microbial biomass carbon content; DOC, dissolved organic carbon content; FRB, fine root biomass; FR-L/N, fine root lignin content: N content; LB, litterfall biomass; L-L/N, litterfall lignin content: N content; BG,  $\beta$ -glucosidase enzyme activities; SC, sucrase enzyme activities; F-Chao1, fungal diversity index; B-Chao1, bacterial diversity index; (Ad/Al) V, acid to aldehyde ratios of the v-type phenols; (Ad/Al) S, acid to aldehyde ratios of the s-type phenols; C/V, C-type phenol content; S/V, S-type phenol content: V-type phenol content.

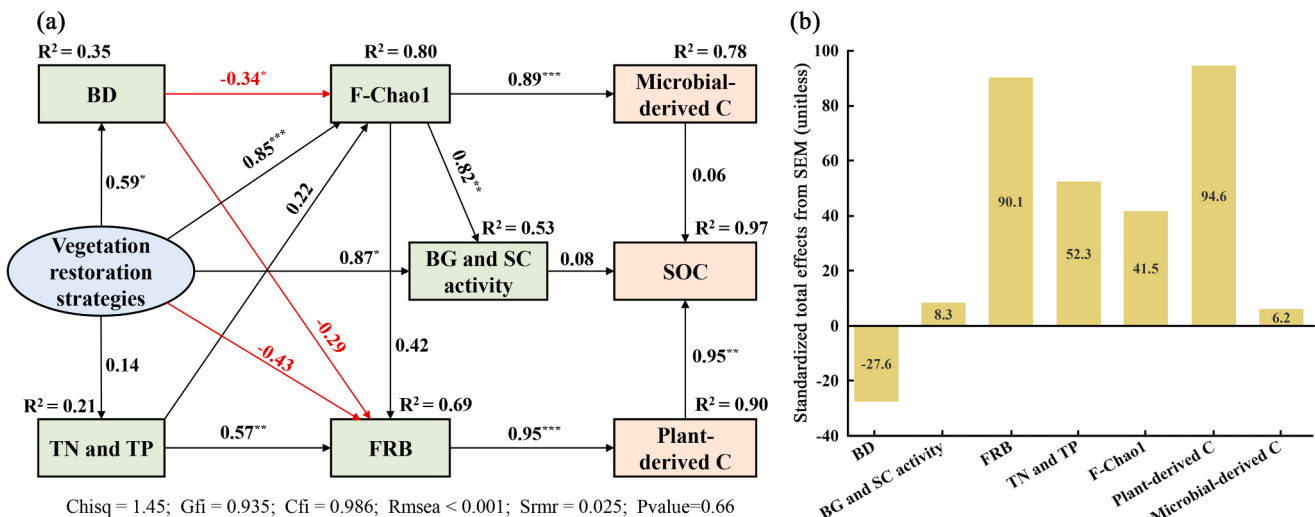


**Fig. 6.** Structural equation modeling (SEM) demonstrating the effects of soil physicochemical properties, plant biomass, microorganisms, and enzymes on the contribution of plant- and microbial-derived C to SOC (a). Standardized total effects of each driver on SOC (b). The number represents the effect size of the relationship. Solid black arrows indicate a positive correlation, and red arrows indicate a negative correlation ( $p < 0.05$ ). Dashed lines indicate indirect effects.  $R^2$  values alongside every variable denote the proportion of variance.

(Sinsabaugh et al., 2013), which enables a greater proportion of C to be incorporated into fungal residues.

#### 4.2. Arbor-shrub mixed and monoculture forests influence lignin phenols and plant-derived C

In our study, the content of total lignin phenol and plant-derived C in the arbor-shrub mixed forests (ApLq and Pcpf) were significantly higher than those in the monoculture forests (Ap and P). Both decreased with

**Table 2**

Soil and plant characteristics of the four vegetation restoration strategies.

Property		Ap	ApLq	Pc	PcPf
Soil 0–10 cm	BD (g cm <sup>-3</sup> )	1.27 ± 0.01 Ba	1.26 ± 0.01 Bb	1.31 ± 0.01 Ab	1.30 ± 0.01 Ab
	pH	7.73 ± 0.26 Aa	7.07 ± 0.31 Ba	7.41 ± 0.14 ABA	7.29 ± 0.34 ABA
	TN (g kg <sup>-1</sup> )	3.13 ± 0.49 Ba	4.53 ± 0.59 Aa	2.73 ± 0.32 Ba	3.60 ± 0.98 ABA
	TC (g kg <sup>-1</sup> )	34.47 ± 5.14 Ba	44.03 ± 1.59 Aa	29.97 ± 5.59 Ba	33.83 ± 4.96 Ba
	TP (g kg <sup>-1</sup> )	1.38 ± 0.44 Aa	1.44 ± 0.16 Aa	1.23 ± 0.15 Aa	1.48 ± 0.36 Aa
	SOC (g kg <sup>-1</sup> )	28.18 ± 0.08 Ca	35.51 ± 0.13 Aa	21.32 ± 0.07 Da	26.92 ± 0.19 Ba
	MBC (mg kg <sup>-1</sup> )	399.84 ± 39.81 ABA	459.12 ± 7.17 Aa	375.12 ± 13.60 Ba	553.00 ± 65.30 Aa
	DOC (mg kg <sup>-1</sup> )	148.68 ± 3.64 Ba	180.72 ± 7.12 Aa	108.48 ± 6.09 Cb	196.16 ± 8.17 Aa
	BG (U g <sup>-1</sup> )	57.10 ± 7.70 ABA	69.37 ± 8.12 Aa	50.84 ± 3.76 Ba	55.00 ± 5.67 Ba
	SC (U g <sup>-1</sup> )	709.70 ± 97.31 Ba	882.34 ± 107.97 Aa	296.27 ± 43.53 Ca	480.84 ± 54.76 BCa
	F-Chao1	402.94 ± 3.66 Ba	450.62 ± 4.48 Aa	380.39 ± 23.57 Da	478.54 ± 37.56 Ca
	B-Chao1	2581.22 ± 59.29 Aa	2763.74 ± 180.12 Aa	2646.79 ± 254.97 Aa	2827.57 ± 55.13 Aa
Soil 10–20 cm	BD (g cm <sup>-3</sup> )	1.37 ± 0.08 ABA	1.33 ± 0.01 Ba	1.43 ± 0.00 Aa	1.41 ± 0.01 ABA
	pH	7.70 ± 0.27 Aa	7.45 ± 0.52 Aa	7.31 ± 0.51 Aa	7.11 ± 0.17 Aa
	TN (g kg <sup>-1</sup> )	2.43 ± 0.06 Ba	3.60 ± 0.36 Aa	2.00 ± 0.30 Bb	2.50 ± 0.20 Ba
	TC (g kg <sup>-1</sup> )	24.87 ± 1.85 BCb	32.63 ± 2.58 Ab	21.53 ± 2.72 Ca	27.47 ± 3.35 Ba
	TP (g kg <sup>-1</sup> )	1.32 ± 0.31 Aa	1.35 ± 0.21 Aa	1.18 ± 0.08 Aa	1.26 ± 0.21 Aa
	SOC (g kg <sup>-1</sup> )	20.57 ± 0.54 Cb	31.77 ± 0.12 Ab	17.12 ± 0.28 Db	21.02 ± 0.11 Bb
	MBC (mg kg <sup>-1</sup> )	359.12 ± 12.98 Ba	417.96 ± 3.55 Ab	325.32 ± 7.72 Cb	352.00 ± 4.46 Bb
	DOC (mg kg <sup>-1</sup> )	92.60 ± 3.39 Bb	108.80 ± 3.23 Ab	109.20 ± 4.67 Aa	115.92 ± 13.30 Ab
	BG (U g <sup>-1</sup> )	41.51 ± 7.35 Bb	51.08 ± 0.16 Ab	36.66 ± 2.88 Ba	43.84 ± 3.16 ABb
	SC (U g <sup>-1</sup> )	570.90 ± 50.21 Ba	784.83 ± 27.78 Aa	60.45 ± 12.60 Db	307.71 ± 57.25 Cb
	F-Chao1	278.94 ± 3.37 Bb	323.05 ± 5.61 Ab	343.95 ± 1.24 Db	385.41 ± 4.25 Cb
	B-Chao1	2492.33 ± 29.10 Aa	2625.26 ± 15.04 Aa	2523.16 ± 30.82 Aa	2662.08 ± 82.07 Aa
Fine roots 0–10 cm	FRB (t ha <sup>-1</sup> )	1.57 ± 0.51 Ba	3.33 ± 0.76 Aa	1.05 ± 0.12 Ba	1.74 ± 0.01 Ba
	FR-N (g kg <sup>-1</sup> )	7.90 ± 0.14 Ca	9.97 ± 0.19 Aa	8.93 ± 0.03 Ba	10.15 ± 0.17 Aa
	FR-C (g kg <sup>-1</sup> )	461.46 ± 0.10 Ca	473.16 ± 0.28 Ba	456.67 ± 0.32 Da	489.32 ± 0.25 Aa
	FR-Lignin (mg g <sup>-1</sup> )	197.79 ± 0.85 Aa	182.67 ± 0.33 Ba	168.72 ± 0.31 Cb	153.60 ± 0.50 Db
	FR-Lignin/N	0.025 ± 0.0003 Aa	0.018 ± 0.0003 Cb	0.019 ± 0.0001 Bb	0.015 ± 0.0003 Db
Fine roots 10–20 cm	FRB (t ha <sup>-1</sup> )	0.98 ± 0.14 Ba	1.83 ± 0.24 Ab	0.42 ± 0.15 Cb	0.81 ± 0.13 Bb
	FR-N (g kg <sup>-1</sup> )	7.67 ± 0.15 Ca	8.04 ± 0.11 Bb	7.32 ± 0.18 Db	9.02 ± 0.17 Ab
	FR-C (g kg <sup>-1</sup> )	454.04 ± 0.13 Db	467.65 ± 0.28 Bb	457.05 ± 0.10 Ca	477.93 ± 0.09 Ab
	FR-Lignin (mg g <sup>-1</sup> )	171.03 ± 0.68 Bb	166.94 ± 0.18 Cb	177.03 ± 0.13 Aa	159.94 ± 0.22 Da
	FR-Lignin/N	0.022 ± 0.0004 Bb	0.021 ± 0.0003 Ca	0.024 ± 0.0006 Aa	0.018 ± 0.0004 Da
Litterfall	LB (t ha <sup>-1</sup> )	3.63 ± 0.23 D	5.03 ± 0.60 C	8.65 ± 0.39 B	9.61 ± 0.07 A
	L-N (g kg <sup>-1</sup> )	7.17 ± 1.20 A	9.10 ± 3.97 A	9.33 ± 0.64 A	10.40 ± 1.80 A
	L-C (g kg <sup>-1</sup> )	458.93 ± 9.35 A	451.23 ± 5.00 A	458.63 ± 18.65 A	455.70 ± 0.72 A
	L-Lignin (mg g <sup>-1</sup> )	170.44 ± 0.14 C	156.29 ± 0.20 D	231.17v0.38 A	176.89 ± 0.30 B
	L-Lignin/N	0.024 ± 0.004 A	0.019 ± 0.007 A	0.025 ± 0.002 A	0.017 ± 0.003 A

Note: BD, soil bulk density; pH, soil pH; TC, soil total carbon content; TN, soil total nitrogen content; TP, total phosphorus content; SOC, soil organic carbon content; MBC, microbial biomass carbon content; DOC, dissolved organic carbon content; FRB, fine root biomass; FR-N, fine root nitrogen content; FR-C, fine root carbon content; FR-Lignin, fine root lignin content; FR-lignin/N, fine root lignin content: N content; LB, litterfall biomass; L-N, litterfall nitrogen content; L-C, litterfall carbon content; L-Lignin, litterfall lignin content; L-lignin/N, litterfall lignin content: N content; BG, β-glucosidase enzyme activities; SC, sucrase enzyme activities; F-Chao1, fungal diversity index; B-Chao1, bacterial diversity index. Different lowercase letters indicate significant differences between different soil layers of the same vegetation type, and different capital letters indicate significant differences between different vegetation types in the same soil layer ( $p < 0.05$ ). Ap, *Acer pictum* monoculture forest; ApLq, *Acer pictum* × *Ligustrum quihoui* mixed forest; Pc, *Pistacia chinensis* monoculture forest; PcPf, *Pistacia chinensis* × *Pyracantha fortuneana* mixed forest.

increasing soil depth (Fig. 3). Arbor-shrub mixed forests improved soil stoichiometric balance and reduced BD, thereby enhancing soil porosity and facilitating water and gas exchange (Eldridge and Delgado-Baquerizo, 2016). These favorable soil conditions promoted root growth (Coonan et al., 2020), increased fine root biomass, and contributed to the accumulation of plant detritus, ultimately leading to higher lignin phenol concentrations (Xia et al., 2022). Furthermore, root growth stimulates the production of root exudates and rhizospheric inputs (Duchene et al., 2017) that likely contribute to the accumulation of more persistent forms of plant-derived C in the soil (Liang et al., 2017). Conversely, soil microorganisms rely on extracellular enzymes to acquire essential nutrients, such as C, N, and P, to sustain their metabolism (Coonan et al., 2020). BG and SC enzymes are crucial for the degradation of lignocellulose and sucrose (Sinsabaugh and Follstad Shah, 2011). Arbor-shrub mixed forests effectively enhanced the activities of BG and SC enzymes, which increased microbial biomass and diversity (Wang et al., 2022; Yang et al., 2022). These enzymes not only directly facilitated lignin phenol formation but also indirectly promoted lignin phenol and plant-derived C accumulation by mediating plant humus decomposition and altering the soil stoichiometry (Hu et al., 2024).

Our study also revealed that the litter inputs, fine root biomass, and

easily decomposable organic C (e.g., DOC) in the 10–20 cm soil layer were substantially lower than those in the 0–10 cm layer (Button et al., 2022). The underlying cause of this outcome stems from the limited availability of fresh plant substrates within the subsoil. Consequently, microorganisms display a heightened propensity to utilize citrate or partially protected plant-derived C particles (Huang et al., 2023). This metabolic preference subsequently results in a reduction in the abundance of lignin phenols and plant-derived carbon in the subsoil.

The ratios of (Ad/AI) V and (Ad/AI) S reflect the extent of microbial activity and lignin oxidation in soils (Sokol et al., 2019), while the ratios of C/V and S/V indicate the degree of lignin decomposition and transformation (Chen et al., 2021). In this study, (Ad/AI) S exhibited a significant negative correlation with SOC and lignin phenols, whereas (Ad/AI) V showed no significant correlation with these variables. Moreover, the C/V and S/V ratios were significantly negatively correlated with amino sugars, FNC, DOC, and MBC (Fig. 5). These findings diverge from the conclusions of Zhu et al. (2024) and Ma et al. (2018) but align with those of Li et al. (2024). The relatively low (Ad/AI) S ratios observed in the ApLq and PcPf forest stands suggest that less lignin was decomposed, thereby promoting the accumulation of lignin phenols. This underscores the contribution of plant-derived C to SOC. In

addition, the reduced C/V and S/V ratios in the ApLq and PcPf forest stands imply that microbial transformation in arbor-shrub mixed ecosystems reached an advanced stage (Dai et al., 2022; Zhu et al., 2024). This observation further explains the increased levels of amino sugars, FNC, and microbial-derived C in the ApLq and PcPf stands.

#### 4.3. Accumulation of SOC mediated by plant- and microbial-derived C under different vegetation restoration strategies

In this study, the contribution of plant-derived C to SOC exhibited a notable increase of 10.18 % and 4.98 % in the ApLq and PcPf stands compared with the Ap and Pc stands, respectively, when compared to the corresponding Ap and Pc stands. In contrast, the proportion of microbial-derived C decreased by 9.39 % and 1.05 % in these stands. Moreover, our previous research unequivocally demonstrated that arbor-shrub mixed forests significantly enhanced both the storage and stability of SOC compared with monoculture forests (Shi et al., 2025). Based on these findings, it can be reasonably concluded that arbor-shrub mixed forests induce a greater increase in plant-derived C relative to microbial-derived C. Furthermore, plant-derived C exerts a more pronounced influence on SOC sequestration in arbor-shrub mixed forests compared to monoculture forests.

The elevated increases in plant-derived C can be attributed to the augmented quantity and enhanced quality of plant organic matter inputs derived from litterfall and fine root turnover, as revealed in Table 2. The heightened influx of high-quality organic matter is likely to have promoted an increase in particulate organic matter (POM), a critical constituent of the soil C pool (Cotrufo et al., 2019). Under the influence of lower soil pH, microbial decomposition of POM may be impeded (Angst et al., 2021). This inhibition allows for a greater proportion of POM to be preserved within soil aggregates or adsorbed onto soil mineral surfaces. Consequently, this stabilization mechanism is presumed to have facilitated the long-term accrual of plant-derived C within the SOC pool.

The plausible explanation for the increase in microbial-derived C content, albeit to a relatively small extent, is that the arbor-shrub mixed forests fostered advantageous soil conditions that promoted microbial proliferation rather than the accumulation of microbial residues. These conditions encompassed lower C/N ratios and BD and elevated TN and TP levels (Chen et al., 2024a). Such favorable edaphic factors collectively facilitated microbial proliferation, augmented MBC accumulation, and boosted soil enzyme activities, as evidenced by Li et al. (2023) and Yuan et al. (2021). Moreover, these conditions prompted a shift in the soil C/P ratio, thereby altering the microbial community composition (Shen et al., 2019). However, despite these propitious soil attributes, the efficiency of carbon (C) transfer from living microbial biomass to microbial necromass was compromised, as proposed by Xu et al. (2022). This impaired conversion efficiency ultimately resulted in a diminished contribution of microbial residues to SOC.

SEM demonstrated that the accumulation of SOC in limestone hills is synergistically regulated by plant-derived C and microbial-derived C. Notably, the standardized total effect value of plant-derived C on SOC was found to be higher, indicating its dominant role in driving SOC variations across different vegetation restoration strategies. This conclusion diverges from the majority of previous studies (Hao et al., 2025; He et al., 2024; Hu et al., 2024; Zhao et al., 2024), although it is congruent with the findings of Dai et al. (2022) and Li et al. (2024). A potential mechanistic explanation for this outcome lies in the fact that the input of plant-derived substrates serves as a fundamental prerequisite for microbial metabolic processes and the accrual of organic carbon in soil (Feng, 2022; Zhao et al., 2024). Arbor-shrub mixed forests significantly augmented both the quantity and quality of plant substrates. This enhancement stimulated the growth and enhanced the diversity of fungi and bacteria (Schulte-Uebbing et al., 2022). Consequently, these changes led to an increase of plant-derived C via ex vivo modification of soil microorganisms (Liang et al., 2017). In addition, a substantial proportion of plant-derived compounds, which act as

substrates for microbial metabolism, remains unutilized. Instead, these compounds are sequestered through stabilization mechanisms, including physical entrapment within soil aggregates or adsorption onto soil mineral surfaces (Sokol and Bradford, 2019; Angst et al., 2023; Zhou et al., 2024). The quantity and extent of protection of this unutilized plant-derived C are pivotal determinants of both the magnitude and long-term stability of SOC pools (Dai et al., 2022). Thus, while microbial processes are indispensable for SOC formation (Liang, 2020; Liang and Zhu, 2021), the characteristics and fate of unprocessed plant-derived C may exert a more profound influence on the persistence and scalability of SOC pools within arbor-shrub mixed forests.

In all forests, the contribution of FNC to SOC exceeded that of BNC to SOC (Fig. 4), which is consistent with the findings of most previous studies (Hao et al., 2025; Li et al., 2022; Li et al., 2024). This is primarily due to differences in the cell wall composition, with the thin bacterial cell walls predominantly composed of easily degradable peptidoglycan and the fungal cell walls predominantly composed of chitin, which is a more recalcitrant and stable compound compared with peptidoglycan (Coonan et al., 2020). Following microbial death, bacterial residues are readily decomposed and recycled by soil microorganisms, while fungal residues degrade more slowly, resulting in longer-term retention within the soil (Fernandez et al., 2016; Jones et al., 2019).

While the predominance of FNC over BNC in the soil C pool is well-documented, our study revealed a significant increase in the contribution of BNC in the mixed arbor-shrub forests (ApLq and PcPf) of 3.08 % and 1.26 % compared to the monoculture forests (Ap and Pc), respectively. In contrast, the contribution of FNC decreased. This shift is likely linked to the greater quantity and higher quality of plant-derived C inputs in the mixed forests (Table 2). Many bacterial groups, such as Actinobacteria and Proteobacteria, are classified as r-strategists, which are characterized by rapid growth in response to the increased availability of labile nutrients (Yang et al., 2023). Such enhanced resource availability in ApLq and PcPf forests promoted bacterial proliferation and accelerated the formation of BNC (Hao et al., 2025). Furthermore, bacterial growth is more sensitive to N availability (Wang et al., 2021) and soil pH (Xu et al., 2022). Thus, the higher TN and lower pH in the mixed forests enhanced N availability and provided favorable conditions for bacterial growth. Additionally, bacterial enzymes are particularly efficient at degrading plant substrates with relatively low lignin content (Cotrufo et al., 2013), further facilitating the incorporation of bacterial residues into SOC. These factors collectively contributed to the increased contribution of BNC to SOC in the mixed arbor-shrub forest systems.

## 5. Conclusions

This study underscores the pronounced advantages of arbor-shrub mixed forests compared to monoculture forests in limestone hills, particularly with respect to promoting the accumulation of soil lignin phenol, plant-derived C, amino sugar, FNC, BNC, microbial-derived C, and SOC. Our results revealed that arbor-shrub mixed vegetation restoration strategies elicited a more pronounced increase in plant-derived C compared to microbial-derived C in limestone hills. Plant-derived C plays a pivotal role in the formation of a stable SOC pool. Moreover, soil bulk density, total nitrogen and phosphorus content, fine root biomass, fungal diversity, and  $\beta$ -glucosidase and sucrase enzyme activity serve as critical mediators influencing the accumulation of plant- and microbial-derived C. Based on these findings, we advocate prioritizing arbor-shrub mixed vegetation restoration strategies when implementing afforestation and ecological restoration practices in limestone hills. This approach is anticipated to enhance SOC sequestration, thereby providing a sustainable solution for vegetation restoration in challenging ecological settings.

## CRediT authorship contribution statement

Hongbo Tao: Investigation. Linjing Zhang: Visualization, Software.

**Junjie Li:** Visualization. **Jiahao Zhao:** Visualization, Data curation. **Xinli Chen:** Writing – review & editing. **Chenyi Yu:** Writing – review & editing, Software. **Qingwei Guan:** Writing – review & editing, Resources, Project administration, Funding acquisition. **Tiandong Xu:** Software, Conceptualization. **Longyan Shi:** Writing – original draft, Visualization, Methodology, Formal analysis. **Yutian Zhang:** Visualization, Conceptualization.

## Declaration of Competing Interest

The authors declare no conflict of interest.

## Acknowledgements

This study was supported by the Jiangsu Carbon Peak Carbon Neutral Science and Technology Innovation Project (BE2022420).

## Data availability

No data was used for the research described in the article.

## References

- Angst, G., Mueller, K.E., Nierop, K.G.J., et al., 2021. Plant- or microbial-derived? A review on the molecular composition of stabilized soil organic matter. *Soil Biol. Biochem.* 156, 10819.
- Angst, G., Mueller, K.E., Castellano, M.J., et al., 2023. Unlocking complex soil systems as carbon sinks: multi-pool management as the key. *Nat. Commun.* 14 (1), 2967.
- Bao, S.D., 2000. Soil Agrochemical Analysis (3rd Ed.). China Agriculture Press, Beijing.
- Bradford, M.A., Keiser, A.D., Davies, C.A., et al., 2013. Empirical evidence that soil carbon formation from plant inputs is positively related to microbial growth. *Biogeochemistry* 113, 271–281.
- Button, E.S., Pett-Ridge, J., Murphy, D.V., et al., 2022. Deep-C storage: Biological, chemical and physical strategies to enhance carbon stocks in agricultural subsoils. *Soil Biol. Biochem.* 170, 108697.
- Castellano, M.J., Mueller, K.E., Olk, D.C., et al., 2015. Integrating plant litter quality, soil organic matter stabilization, and the carbon saturation concept. *Glob. Change Biol.* 21 (9), 3200–3209.
- Chen, L., Zhou, G.X., Feng, B., et al., 2024b. Saline-alkali land reclamation boosts topsoil carbon storage by preferentially accumulating plant-derived carbon. *Sci. Bull.* 69, 2948–2958.
- Chen, X., Hu, Y., Xia, Y., et al., 2021. Contrasting pathways of carbon sequestration in paddy and upland soils. *Glob. Change Biol.* 27 (11), 2478–2490.
- Chen, X., Reich, P.B., Taylor, A.R., et al., 2024a. Resource availability enhances positive tree functional diversity effects on carbon and nitrogen accrual in natural forests. *Nat. Commun.* 15 (1), 8615.
- Coonan, E.C., Kirkby, C.A., Kirkegaard, J.A., et al., 2020. Microorganisms and nutrient stoichiometry as mediators of soil organic matter dynamics. *Nutr. Cycl. Agroecosyst.* 117 (3), 273–298.
- Córdoba, S.C., Olk, D.C., Dietzel, R.N., et al., 2018. Plant litter quality affects the accumulation rate, composition, and stability of mineral-associated soil organic matter. *Soil Biol. Biochem.* 125, 115–124.
- Cotrufo, M.F., Wallenstein, M.D., Boot, C.M., et al., 2013. The Microbial Efficiency-Matrix Stabilization (MEMS) framework integrates plant litter decomposition with soil organic matter stabilization: do labile plant inputs form stable soil organic matter? *Glob. Change Biol.* 19 (4), 988–995.
- Cotrufo, M.F., Ranalli, M.G., Haddix, M.L., et al., 2019. Soil carbon storage informed by particulate and mineral-associated organic matter. *Nat. Geosci.* 12 (12), 989–994.
- Dai, G., Zhu, S., Cai, Y., et al., 2022. Plant-derived lipids play a crucial role in forest soil carbon accumulation. *Soil Biol. Biochem.* 168, 108645.
- Delgado-Baquerizo, M., Bissett, A., Eldridge, D.J., et al., 2017. Palaeoclimate explains a unique proportion of the global variation in soil bacterial communities. *Nat. Ecol. Evol.* 1 (9), 1339–1347.
- Deng, S., Zheng, X., Chen, X., et al., 2021. Divergent mineralization of hydrophilic and hydrophobic organic substrates and their priming effect in soils depending on their preferential utilization by bacteria and fungi. *Biol. Fertil. Soils* 57, 65–76.
- Ding, X., Chen, S., Zhang, B., et al., 2020. Warming yields distinct accumulation patterns of microbial residues in dry and wet alpine grasslands on the Qinghai-Tibetan Plateau. *Biol. Fertil. Soils* 56, 881–892.
- Dong, W., Hu, C., Chen, S., et al., 2009. Tillage and residue management effects on soil carbon and CO<sub>2</sub> emission in a wheat-corn double-cropping system. *Nutr. Cycl. Agroecosyst.* 83, 27–37.
- Duboc, O., Dignac, M.F., Djukic, I., et al., 2014. Lignin decomposition along an Alpine elevation gradient in relation to physicochemical and soil microbial parameters. *Glob. Change Biol.* 20 (7), 2272–2285.
- Duchene, O., Vian, J.F., Celette, F., 2017. Intercropping with legume for agroecological cropping systems: complementarity and facilitation processes and the importance of soil microorganisms. A review. *Agric. Ecosyst. Environ.* 240, 148–161.
- Edgar, R.C., 2013. UPARSE: highly accurate OTU sequences from microbial amplicon reads. *Nat. Methods* 10 (10), 996–998.
- Eldridge, D.J., Delgado-Baquerizo, M., 2016. Continental-scale impacts of livestock grazing on ecosystem supporting and regulating services. *Land Degrad. Dev.* 28 (4), 1473–1481.
- Feng, X., 2022. Plant influences on soil organic carbon dynamics. *CABI Digit. Libr.* 47–82.
- Feng, X., Simpson, M.J., 2007. The distribution and degradation of biomarkers in Alberta grassland soil profiles. *Org. Geochem.* 38 (9), 1558–1570.
- Feng, X., Dai, G., Liu, T., et al., 2024. Understanding the mechanisms and potential pathways of soil carbon sequestration from the biogeochemistry perspective. *Sci. China Earth Sci.* 67 (11), 3386–3396.
- Fernandez, C.W., Langley, J.A., Chapman, S., et al., 2016. The decomposition of ectomycorrhizal fungal necromass. *Soil Biol. Biochem.* 93, 38–49.
- Fu, Y., Luo, Y., Tang, C., et al., 2022. Succession of the soil bacterial community as resource utilization shifts from plant residues to rhizodeposits. *Soil Biol. Biochem.* 173, 108785.
- Gunina, A., Kuzyakov, Y., 2022. From energy to (soil organic) matter. *Glob. Change Biol.* 28 (7), 2169–2182.
- Haghverdi, K., Kooch, Y., 2019. Effects of diversity of tree species on nutrient cycling and soil-related processes[J]. *Catena* 178, 335–344.
- Han, B., Yao, Y., Wang, Y., et al., 2024. Microbial traits dictate soil necromass accumulation coefficient: A global synthesis. *Glob. Ecol. Biogeogr.* 33 (1), 151–161.
- Hao, H., Wang, R., Li, S., et al., 2025. Different contributions of microbial and plant residues to soil organic carbon accumulation during planted forest and abandoned farmland restoration, Loess Plateau, China. *Plant Soil* 507 (1), 845–862.
- He, J., Nie, Y., Tan, X., et al., 2024. Latitudinal patterns and drivers of plant lignin and microbial necromass accumulation in forest soils: Disentangling microbial and abiotic controls. *Soil Biol. Biochem.* 194, 109438.
- He, X., Sheng, M., Wang, L., et al., 2022. Effects on soil organic carbon accumulation and mineralization of long-term vegetation restoration in Southwest China karst. *Ecol. Indic.* 145, 109622.
- Hedges, J.I., Ertel, J.R., 1982. Characterization of lignin by gas capillary chromatography of cupric oxide oxidation products. *Anal. Chem.* 54 (2), 174–178.
- Hu, H., Qian, C., Xue, K., et al., 2024. Reducing the uncertainty in estimating soil microbial-derived carbon storage. *Proc. Natl. Acad. Sci.* 121 (35), e2401916121.
- Hu, Y., Zheng, Q., Noll, L., et al., 2020. Direct measurement of the in situ decomposition of microbial-derived soil organic matter. *Soil Biol. Biochem.* 141, 107660.
- Huang, W., Kuzyakov, Y., Niu, S., et al., 2023. Drivers of microbially and plant-derived carbon in topsoil and subsoil. *Glob. Change Biol.* 29 (22), 6188–6200.
- Jenkinson D.S. Determination of microbial biomass carbon and nitrogen in soil[J]. Advances in nitrogen cycling in agricultural systems. Ed. J.R. Wilson. Wallingford: CABI, 1988: 368–386.
- Jia, Y., Zhai, G., Zhu, S., et al., 2021. Plant and microbial pathways driving plant diversity effects on soil carbon accumulation in subtropical forest. *Soil Biol. Biochem.* 161, 108375.
- Jing, Y., Li, X., Zhang, Y., et al., 2024. Effects of thinning on accumulation of soil microbial residue carbon of *Picea asperata* plantations in sub-alpine region of western Sichuan, China. *Chin. J. Appl. Ecol.* 35 (1), 169–176.
- Joergensen, R.G., 2018. Amino sugars as specific indices for fungal and bacterial residues in soil. *Biol. Fertil. Soils* 54, 559–568.
- Jones, D.L., Cooledge, E.C., Hoyle, F.C., et al., 2019. pH and exchangeable aluminum are major regulators of microbial energy flow and carbon use efficiency in soil microbial communities. *Soil Biol. Biochem.* 138, 107584.
- Kallenbach, C.M., Frey, S.D., Grandy, A.S., 2016. Direct evidence for microbial-derived soil organic matter formation and its ecophysiological controls. *Nat. Commun.* 7 (1), 13630.
- Klindworth, A., Pruesse, E., Schweer, T., et al., 2013. Evaluation of general 16S ribosomal RNA gene PCR primers for classical and next-generation sequencing-based diversity studies. *Nucleic Acids Res.* 41 (1), e1–e11.
- Lal, R., Monger, C., Nave, L., et al., 2021. The role of soil in regulation of climate. *Philos. Trans. R. Soc. B* 376 (1834), 20210084.
- Lange, M., Eisenhauer, N., Sierra, C.A., et al., 2015. Plant diversity increases soil microbial activity and soil carbon storage. *Nat. Commun.* 6 (1), 6707.
- Lavallee, J.M., Soong, J.L., Cotrufo, M.F., 2020. Conceptualizing soil organic matter into particulate and mineral-associated forms to address global change in the 21st century. *Glob. Change Biol.* 26 (1), 261–273.
- Li, J., Dong, L., Fan, M., et al., 2024. Long-term vegetation restoration promotes lignin phenol preservation and microbial anabolism in forest plantations: Implications for soil organic carbon dynamics. *Sci. Total Environ.* 928 (10), 172635.
- Li, T., Wu, S., Wang, L., et al., 2022. Progress in national and international research on mixed forest. *World Forestry. Research* 35 (5), 42–48.
- Li, T., Yuan, Y., Mou, Z., et al., 2023. Faster accumulation and greater contribution of glomalin to the soil organic carbon pool than amino sugars do under tropical coastal forest restoration. *Glob. Change Biol.* 29 (2), 533–546.
- Liang, C., 2020. Soil microbial carbon pump: Mechanism and appraisal. *Soil Ecol. Lett.* 2 (4), 241–254.
- Liang, C., Zhu, X., 2021. The soil microbial carbon pump as a new concept for terrestrial carbon sequestration. *Sci. China Earth Sci.* 64, 545–558.
- Liang, C., Schimel, J.P., Jastrow, J.D., 2017. The importance of anabolism in microbial control over soil carbon storage. *Nat. Microbiol.* 2 (8), 1–6.
- Liang, C., Amelung, W., Lehmann, J., et al., 2019. Quantitative assessment of microbial necromass contribution to soil organic matter. *Glob. Change Biol.* 25 (11), 3578–3590.

- Liu, X., Zhang, X., Liu, Y., et al., 2020. Effects of vegetation restoration on the species composition and diversity of plant communities in the limestone mountains in northern Anhui Province. *Pratacult. Sci.* 37 (5), 845–852.
- Luo, X., Zhang, L., Lin, Y., et al., 2023. Nitrogen availability mediates soil organic carbon cycling in response to phosphorus supply: a global meta-analysis. *Soil Biol. Biochem.* 185, 109158.
- Ma, T., Zhu, S., Wang, Z., et al., 2018. Divergent accumulation of microbial necromass and plant lignin components in grassland soils. *Nat. Commun.* 9 (1), 3480.
- Miltner, A., Bombach, P., Schmidt-Bücken, B., et al., 2012. SOM genesis: microbial biomass as a significant source. *Biogeochemistry* 111, 41–55.
- Otto, A., Simpson, M.J., 2005. Degradation and preservation of vascular plant-derived biomarkers in grassland and forest soils from Western Canada. *Biogeochemistry* 74, 377–409.
- Otto, A., Simpson, M.J., 2006. Sources and composition of hydrolysable aliphatic lipids and phenols in soils from western Canada. *Org. Geochem.* 37 (4), 385–407.
- Pretzsch, H., Schütze, G., 2016. Effect of tree species mixing on the size structure, density, and yield of forest stands. *Eur. J. For. Res.* 135, 1–22.
- Qin, G., He, W., Sanders, C., et al., 2024a. Contributions of plant-and microbial-derived residuals to mangrove soil carbon stocks: implications for blue carbon sequestration. *Funct. Ecol.* 38 (3), 573–585.
- Qin, Z., Liu, R., He, P., et al., 2024b. Effects of mixed broadleaved tree species with pure *Pinus massoniana* plantation on soil microbial necromass carbon and organic carbon fractions. *Chin. J. Appl. Ecol.* 35 (1), 141–152.
- Richards, A.E., Forrester, D.I., Bauhus, J., et al., 2010. The influence of mixed tree plantations on the nutrition of individual species: a review. *Tree Physiol.* 30 (9), 1192–1208.
- Schulte-Uebbing, L.F., Ros, G.H., de Vries, W., 2022. Experimental evidence shows minor contribution of nitrogen deposition to global forest carbon sequestration. *Glob. Change Biol.* 28 (3), 899–917.
- Shao, P., Liang, C., Lynch, L., et al., 2019. Reforestation accelerates soil organic carbon accumulation: Evidence from microbial biomarkers. *Soil Biol. Biochem.* 131, 182–190.
- Shao, S., Wang, Z., Pan, L., et al., 2024. Effects of *Phyllostachys edulis* expansion on soil microbial residue carbon accumulation in evergreen broad-leaved forests. *J. Zhejiang A F. Univ.* 41 (5), 1005–1012.
- Shen, F., Wu, J., Fan, H., et al., 2019. Soil N/P and C/P ratio regulate the responses of soil microbial community composition and enzyme activities in a long-term nitrogen loaded Chinese fir forest. *Plant Soil* 436, 91–107.
- Sheng, M., Xiong, K., Wang, L., et al., 2018. Response of soil physical and chemical properties to rocky desertification succession in South China Karst. *Carbonate Evaporite* 33, 15–28.
- Shi, L., Zhang, Y., Zhang, L., et al., 2025. Arbor-shrub mixed vegetation restoration strategies enhanced soil organic carbon storage and stability via fine root and fungal characteristics in limestone hills. *Plant Soil* 1–18.
- Sinsabaugh, R.L., Follstad Shah, J.J., 2011. Ecoenzymatic stoichiometry of recalcitrant organic matter decomposition: the growth rate hypothesis in reverse. *Biogeochemistry* 102, 31–43.
- Sinsabaugh, R.L., Manzoni, S., Moorhead, D.L., et al., 2013. Carbon use efficiency of microbial communities: stoichiometry, methodology and modelling. *Ecol. Lett.* 16 (7), 930–939.
- Sokol, N.W., Bradford, M.A., 2019. Microbial formation of stable soil carbon is more efficient from belowground than aboveground input. *Nat. Geosci.* 12 (46), 53.
- Sokol, N.W., Sanderman, J., Bradford, M.A., 2019. Pathways of mineral-associated soil organic matter formation: Integrating the role of plant carbon source, chemistry, and point of entry. *Glob. Change Biol.* 25 (1), 12–24.
- Wang, B., An, S., Liang, C., et al., 2021. Microbial necromass as the source of soil organic carbon in global ecosystems. *Soil Biol. Biochem.* 162, 108422.
- Wang, M., Dungait, J.A.J., Wei, X., et al., 2022. Long-term warming increased microbial carbon use efficiency and turnover rate under conservation tillage system. *Soil Biol. Biochem.* 172, 108770.
- Whalen, E.D., Grandy, A.S., Sokol, N.W., et al., 2022. Clarifying the evidence for microbial- and plant-derived soil organic matter, and the path toward a more quantitative understanding. *Glob. Change Biol.* 28 (24), 7167–7185.
- Wu, H., Cui, H., Fu, C., et al., 2024. Unveiling the crucial role of soil microorganisms in carbon cycling: a review. *Sci. Total Environ.* 909, 168627.
- Xia, S., Song, Z., Li, Q., et al., 2021. Distribution, sources, and decomposition of soil organic matter along a salinity gradient in estuarine wetlands characterized by C: N ratio, δ<sup>13</sup>C-δ<sup>15</sup>N, and lignin biomarker. *Glob. Change Biol.* 27 (2), 417–434.
- Xia, S., Song, Z., Van Zwieten, L., et al., 2022. Storage, patterns and influencing factors for soil organic carbon in coastal wetlands of China. *Glob. Change Biol.* 28 (20), 6065–6085.
- Xia, Y., Chen, X., Zheng, X., et al., 2020. Preferential uptake of hydrophilic and hydrophobic compounds by bacteria and fungi in upland and paddy soils. *Soil Biol. Biochem.* 148, 107879.
- Xu, Y., Gao, X., Liu, Y., et al., 2022. Differential accumulation patterns of microbial necromass induced by maize root vs. shoot residue addition in agricultural Alfisols. *Soil Biol. Biochem.* 164, 108474.
- Yang, Y., Dou, Y., Wang, B., et al., 2023. Deciphering factors driving soil microbial life-history strategies in restored grasslands. *iMeta* 2 (1), e66.
- Yang, Y., Wang, B., Dou, Y., et al., 2024. Advances in the research of transformation and stabilization of soil organic carbon from plant and microbe. *Chin. J. Appl. Ecol.* 35 (1), 111–123.
- Yang, Z., Zhang, Y., Wang, Y., et al., 2022. Intercropping regulation of soil phosphorus composition and microbially-driven dynamics facilitates maize phosphorus uptake and productivity improvement. *Field Crops Res.* 287, 108666.
- Yuan, Y., Li, Y., Mou, Z., et al., 2021. Phosphorus addition decreases microbial residual contribution to soil organic carbon pool in a tropical coastal forest. *Glob. Change Biol.* 27 (2), 454–466.
- Zhang, H., Luo, G., Wang, Y., et al., 2023. Crop rotation-driven change in physicochemical properties regulates microbial diversity, dominant components, and community complexity in paddy soils. *Agric. Ecosyst. Environ.* 343, 108278.
- Zhang, Q., Jia, X., Li, T., et al., 2022. Forest expansion on cropland on China's Loess Plateau facilitates C sequestration by increasing microbial-derived but not plant-derived carbohydrates. *Catena* 211, 106019.
- Zhang, X., Ma, Y., Fu, S., et al., 2024. Effect and mechanisms of conifer and broadleaf mixtures on the soil characteristics in limestone mountains. *Turk. J. Agric. For.* 48 (2), 199–211.
- Zhao, X., Tian, P., Zhang, W., et al., 2024. Nitrogen deposition caused higher increases in plant-derived Carbon than microbial-derived Carbon in forest soils. *Sci. Total Environ.* 925, 171752.
- Zhou, Z., Liu, L., Hou, L., et al., 2022. Soil organic carbon stabilization and formation: mechanism and model. *J. Beijing For. Univ.* 44 (10), 11–22.
- Zhou, Z., Ren, C., Wang, C., et al., 2024. Global turnover of soil mineral-associated and particulate organic carbon. *Nat. Commun.* 15 (1), 5329.
- Zhu, M., Fanin, N., Wang, Q., et al., 2024. High functional breadth of microbial communities decreases home-field advantage of litter decomposition[J]. *Soil Biol. Biochem.* 188, 109232.
- Zhu, Q., Yang, Z., Zhang, Y., et al., 2024. Intercropping regulates plant- and microbe-derived carbon accumulation by influencing soil physicochemical and microbial physiological properties. *Agric. Ecosyst. Environ.* 364, 108880.

## Glossary

- Ap:* *Acer pictum* subsp. *mono* (Maxim.) H. Ohashi forest  
*Pc:* *Pistacia chinensis* Bunge forest  
*ApLq:* *Acer pictum* × *Ligustrum quihoui* Carr. Forest  
*PcPf:* *Pistacia chinensis* × *Pyracantha fortuneana* (Maxim.) H. L. Li forest  
*SOC:* soil organic carbon  
*MNC:* microbial necromass carbon  
*FNC:* fungal necromass carbon  
*BNC:* bacterial necromass carbon  
*DOC:* dissolved organic carbon  
*(Ad/Al) V:* acid to aldehyde ratios of the v-type phenols  
*(Ad/Al) S:* acid to aldehyde ratios of the s-type phenols  
*GlcN:* glucosamine  
*ManN:* mannosamine  
*GalN:* galactosamine  
*MurA:* muramic acid  
*BD:* soil bulk density  
*BG:* β-glucosidase enzyme  
*SC:* sucrase enzyme  
*TN:* total nitrogen content  
*TC:* total carbon content  
*TP:* total phosphorus content  
*FRB:* fine roots biomass  
*FR-N:* fine roots total nitrogen content  
*FR-C:* fine roots total carbon content  
*FR-Lignin:* fine roots total lignin content  
*FR-lignin/N:* fine root lignin content: TN content  
*LB:* litterfall biomass  
*L-N:* litterfall total nitrogen content  
*L-C:* litterfall total carbon content  
*L-Lignin:* litterfall total lignin content  
*L-lignin/N:* litterfall lignin content: TN content  
*F-Chao 1:* Chao 1 index of fungi  
*B-Chao 1:* Chao 1 index of bacteria  
*SEM:* structural equation modeling  
*DBH:* diameter at breast height